An evolutionarily ancient fatty acid desaturase is required for the synthesis of hexadecatrienoic acid, which is the main source of the bioactive jasmonate in *Marchantia polymorpha*

Gonzalo Soriano[1,2] (iD), Sophie Kneeshaw[1] (iD), Guillermo Jimenez-Aleman[1] (iD), Ángel M. Zamarreño[3] (iD), José Manuel Franco-Zorrilla[1] (iD), Mª Fernanda Rey-Stolle[4] (iD), Coral Barbas[4] (iD), Jose M. García-Mina[3] (iD) and Roberto Solano[1] (iD)

[1]Department of Plant Molecular Genetics, Centro Nacional de Biotecnología, Consejo Superior de Investigaciones Científicas (CNB-CSIC), Madrid 28049, Spain; [2]Facultad de Ciencia y Tecnología, Universidad de La Rioja, Madre de Dios 53, Logroño (La Rioja) 26006, Spain; [3]Department of Environmental Biology, University of Navarra, Navarra 31008, Spain; [4]Centre for Metabolomics and Bioanalysis (CEMBIO), Chemistry and Biochemistry Department, Pharmacy Faculty, Universidad San Pablo-CEU, Boadilla del Monte, Madrid 28668, Spain

Summary

- Jasmonates are fatty acid-derived hormones that regulate multiple aspects of plant development, growth and stress responses. Bioactive jasmonates, defined as the ligands of the conserved COI1 receptor, differ between vascular plants and bryophytes (jasmonoyl-L-isoleucine (JA-Ile) and dinor-12-oxo-10,15(Z)-phytodienoic acid (dn-OPDA), respectively). The biosynthetic pathways of JA-Ile in the model vascular plant *Arabidopsis thaliana* have been elucidated. However, the details of dn-OPDA biosynthesis in bryophytes are still unclear.
- Here, we identify an orthologue of *Arabidopsis* fatty-acid-desaturase 5 (AtFAD5) in the model liverwort *Marchantia polymorpha* and show that FAD5 function is ancient and conserved between species separated by more than 450 million years (Myr) of independent evolution. Similar to AtFAD5, MpFAD5 is required for the synthesis of 7Z-hexadecenoic acid. Consequently, in Mp*fad5* mutants, the hexadecanoid pathway is blocked, dn-OPDA concentrations are almost completely depleted and normal chloroplast development is impaired.
- Our results demonstrate that the main source of wounding-induced dn-OPDA in *Marchantia* is the hexadecanoid pathway and the contribution of the octadecanoid pathway (i.e. from OPDA) is minimal.
- Remarkably, despite extremely low concentrations of dn-OPDA, MpCOI1-mediated responses to wounding and insect feeding can still be activated in Mp*fad5*, suggesting that dn-OPDA may not be the only bioactive jasmonate and COI1 ligand in *Marchantia*.

Introduction

Jasmonates are fatty acid (FA)-derived phytohormones that play a critical role in plant development and survival. They regulate responses to a wide range of stresses, both biotic (e.g. herbivory and necrotrophic pathogen infection) and abiotic (e.g. mechanical wounding, drought or heat; Howe *et al.*, 2018; Wasternack & Feussner, 2018; Monte *et al.*, 2020). Moreover, they are involved in a multitude of developmental processes such as senescence, growth, flower development and fertility (Howe *et al.*, 2018; Wasternack & Feussner, 2018).

Most jasmonate-responsive processes are mediated by the COI1-JAZ coreceptor complex, where coronatine insensitive 1 (COI1) is the F-box component of an E3-type ubiquitin ligase, and jasmonate-ZIM domain (JAZ) proteins are repressors of downstream transcription factors (TFs) (Chini *et al.*, 2007; Thines *et al.*, 2007; Sheard *et al.*, 2010; Howe *et al.*, 2018). During

the activation of jasmonate signaling, a bioactive jasmonate triggers the interaction of COI1 and JAZ by acting as a 'molecular glue' between both proteins, thus forming the coreceptor complex (Katsir *et al.*, 2008; Fonseca *et al.*, 2009; Sheard *et al.*, 2010). Through its interaction with COI1, the JAZ repressor is ubiquitinated and then degraded by the proteasome, resulting in a derepression of jasmonate-related TFs, including the jasmonate-responsive master regulator, MYC2 (Lorenzo *et al.*, 2004; Chini *et al.*, 2007; Fernandez-Calvo *et al.*, 2011; Qi *et al.*, 2015; Chini *et al.*, 2016; Howe *et al.*, 2018). In addition to this, through the electrophilic properties of their cyclopentanone rings, jasmonates also regulate a subset of genes through a COI1-independent pathway. It has recently been shown that this pathway activates heat stress (HS) responses and contributes to basal thermotolerance (Farmer & Mueller, 2013; Monte *et al.*, 2020).

The octadecanoid pathway has been described as the major source of jasmonate biosynthesis in plants (Supporting

Information Fig. S1). α-Linolenic acid (ALA, 18:3n3) is released from chloroplast membranes and subjected to the consecutive actions of lipoxygenase, allene oxide synthase (AOS) and allene oxide cyclase (AOC) enzymes, to produce 12-oxo-phytodienoic acid (OPDA). This compound is transported to the peroxisome where it is converted into jasmonic acid (JA) via OPDA reductase 3 (OPR3)-mediated reduction and three successive rounds of β-oxidation. In some plant species, such as *Arabidopsis thaliana*, a parallel JA biosynthesis route exists, the hexadecanoid pathway, in which hexadecatrienoic acid (HTA, 16:3n3) undergoes the same processing as ALA (18:3n3) to produce a molecule that is structurally similar to OPDA, dinor-12-oxo-phytodienoic acid (dn-OPDA; Fig. S1; Weber *et al.*, 1997). Furthermore, in *Arabidopsis*, analysis of *opr3* mutants elucidated an OPR3-independent pathway in which OPDA suffers three β-oxidations to produce dn-OPDA, tetranor-OPDA (tn-OPDA) and then 4,5-ddh-JA, which is finally reduced to JA by cytoplasmic OPRs (Chini *et al.*, 2018).

In vascular plants, JA is conjugated to L-isoleucine (Ile) by JASMONATE RESISTANT 1 (JAR1), giving rise to the bioactive form of the hormone, (+)-7-*iso*-JA-Ile (JA-Ile; Staswick & Tiryaki, 2004; Thines *et al.*, 2007; Fonseca *et al.*, 2009; Sheard *et al.*, 2010). Bryophytes, however, do not synthesize JA-Ile and dn-OPDA acts as the bioactive jasmonate. Dinor-OPDA binds a conserved COI1-JAZ coreceptor and regulates similar responses to those activated by JA-Ile in vascular plants (Monte *et al.*, 2018, 2019, 2020; Peñuelas *et al.*, 2019).

In plants, the synthesis of polyunsaturated FAs (PUFAs) such as ALA (18:3n3) and HTA (16:3n3) is carried out by a protein family known as FA desaturases (FADs), which introduce a double bond regiospecifically in the FA backbone. These FADs show high substrate specificity and are active in different subcellular compartments such as the endoplasmic reticulum (ER; the eukaryotic pathway) or in the chloroplasts (the prokaryotic pathway) (Aid, 2019; He *et al.*, 2020).

In contrast to ALA (18:3n3), which can be synthesized in both the ER (by FAD3) (Arondel *et al.*, 1992) and the plastids (by FAD7 and FAD8), HTA (16:3n3) is exclusively synthesized in the chloroplast and its production requires a specific FAD, the FAD5 (Weber *et al.*, 1997). In *Arabidopsis*, this enzyme has been described as a plastidial Δ^7-desaturase undertaking the first desaturation of palmitic acid to render 7Z-hexadecenoic acid (HD; a Δ^7-16:1 FA that, in this particular case, matches a 16:1n9) (Heilmann *et al.*, 2004a). After this first dehydrogenation, FAD6 and FAD7/FAD8 undertake two consecutive desaturation reactions to create $\Delta^{7,10}$-hexadecadienoic (HAD, 16:2n6) and HTA (16:3n3), respectively (Browse *et al.*, 1989; Gibson *et al.*, 1994; McConn *et al.*, 1994).

Although the biosynthesis of PUFAs and dn-OPDA has been well studied in vascular plants (Weber *et al.*, 1997; Chini *et al.*, 2018; Aid, 2019; He *et al.*, 2020), details of their production in bryophytes remain to be elucidated. It has been suggested that in bryophytes, as in *Arabidopsis*, dn-OPDA can be synthesized from both octadecanoid and hexadecanoid pathways. Indeed, in the model liverwort *Marchantia polymorpha*, the addition of labelled ALA (18:3n3) or HTA (16:3n3) results in the accumulation of

labelled dn-OPDA (Monte *et al.*, 2018). However, it is unclear if the conversion of ALA/HTA into dn-OPDA occurs *in vivo* in untreated plants, and the enzymes involved in this process have not yet been characterized.

Here, we elucidated the biosynthetic pathway of dn-OPDA in the model bryophyte *Marchantia*. We identified the *Marchantia* orthologue of AtFAD5 and generated a loss-of-function mutant of the Mp*FAD5* gene, which enabled us to perform a comprehensive analysis into the role of HTA (16:3n3) and FAD5 in bryophytes. We show that C16 FAs and FAD5 are essential for proper chloroplast development in C16 plants. Additionally, we further dissected the biosynthetic pathway of the bioactive hormone (defined as the ligand of COI1) in nonvascular plants, namely dn-OPDA. Our data indicate that, although the conversion of OPDA to dn-OPDA may exist in *Marchantia*, the majority of dn-OPDA accumulating after wounding is synthesized from HTA (16:3n3) *de novo* – that is, almost exclusively via the 16:3, and not the 18:3, pathway. In the absence of HTA (16:3n3), dn-OPDA concentrations were extremely low in Mp*fad5* mutants. Surprisingly, however, typical dn-OPDA-mediated environmental stress responses could still be activated in the mutant, indicating either that very low concentrations of dn-OPDA may be sufficient to trigger large parts of the jasmonate response or that other bioactive jasmonates, besides dn-OPDA, may activate the MpCOI1 receptor in *Marchantia*.

Materials and Methods

Plant material

Marchantia polymorpha accession Takaragaike-1 (Tak-1) was used as the wild-type (WT). In this genetic background, we used CRISPR-Cas9$_{D10A}$ nickase-mediated mutagenesis with Mp*FAD5* as the target. The sequence of this gene was obtained from www.marchantia.info. Four different gRNAs were designed flanking the first exon of the gene (Table S3). They were then first cloned into pBC-GE12, pBC-GE23, pBC-GE34 and pMPGE_EN04 vectors, before being subsequently transferred in tandem by LR reaction to the pMpGE018 binary vector carrying the CRISPR-Cas9$_{D10A}$ nickase (Ran *et al.*, 2013; Shen *et al.*, 2014). Using regenerating thalli transformation (Kubota *et al.*, 2013), WT plants were transformed and thalli selected by chlorosulfuron resistance. Then, gDNA of transformants were extracted and sequenced using gRNAs flanking primers (Sugano & Nishihama, 2018). In addition to the mutants generated in this study, Mp*coi1-2* (Monte *et al.*, 2018) was used in some experiments as a control for dn-OPDA insensitivity.

Culture conditions

Plants were routinely grown at 21°C, under continuous white light (50–60 mmol m^{-2} s^{-1}) on Petri plates containing 1% agar half-strength Gamborg's B5 medium. For FA quantification, wounding assays (both hormone measurements and gene expression), Chl extraction and Chl fluorescence measurements, plants were grown for 3 wk.

For the antheridiophore induction experiment, gemmae of WT, Mp*fad5* and Mp*coi1-2* (all in Tak-1 background) were placed in Gamborg's B5 plates and after 10 d they were transferred to soil. At 3 wk after transplant, promotion of antheridiophores was induced by supplementation of white light with far red (Chiyoda *et al.*, 2008; Kubota *et al.*, 2014).

Thalli area, pigment contents and photosynthetic variables

For thalli area measurements, pictures of 3-wk-old plants were taken with a NIKON D1-x camera and the area was measured using IMAGEJ software.

Maximum (F_m) and minimum (F_0) Chl fluorescence values were measured after 21 d of culture, using a portable pulse amplitude modulation fluorometer (MINI-PAM; Walz, Effeltrich, Germany). Then, the maximum quantum yield of PSII (F_v/F_m) was determined, where $F_v = F_m - F_0$.

Photosynthetic pigments were extracted with 95% ethanol after freezing shoot apices in liquid N_2 and grounding them in a TissueLyser (Qiagen). Chl*a* and *b* were quantified by spectrophotometry (Sumanta *et al.*, 2014).

For these variables, four biological replicates, each with three technical replicates, were analysed.

Microscopy analysis of chloroplast

Plants of WT and Mp*fad5-3* at the same developmental stage (after the second thalli bifurcation when the plants have eight apices) were cut into small pieces (1 × 2 mm) and fixed immediately in buffered phosphate 0.1 M paraformaldehyde 4% (Electron Microscopy Sciences, Hatfield, PA, USA) and glutaraldehyde 2.5% (TAAB Laboratories, Aldermaston, UK) for 3 h at room temperature and for 48 h at 4°C. Samples were washed with 0.1 M phosphate buffer, post-fixed (for 1 h at 4°C) with 1% osmium tetroxide (TAAB Laboratories) in potassium ferricyanide 0.8% (Sigma) and incubated with 2% aqueous uranyl acetate (Electron Microscopy Sciences) for 1 h at 4°C. After washing with distilled water, samples were dehydrated with increasing concentrations of acetone (anhydrous, VWR, Radnor, PA, USA) and embedded in epoxy resin TAAB 812 (TAAB Laboratories). Polymerization was carried out (in epoxy resin 100%) for 2 d at 60°C. Resin blocks were trimmed, and ultrathin 70-nm-thick sections were obtained with the Ultracut UC6 ultramicrotome (Leica Microsystems, Wetzlar, Germany), transferred to 200 mesh formvar carbon-coated nickel grids (Gilder, Lincolnshire, UK) and stained with 2% aqueous uranyl acetate (for 30 min) and lead citrate 0.2% (for 1 min) at room temperature. Sections were visualized on a Jeol JEM 1011 electron microscope operating at 100 kV (Tokyo, Japan). Micrographs were taken with a Gatan Erlangshen ES1000W digital camera (Pleasanton, CA, USA) at various magnifications.

Phytohormone and FA measurements

Three-week-old thalli of the WT and Mp*fad5-3* and *Mpfad5-8* mutants were mechanically wounded with tweezers, pressing with them all over the thallus surface (Monte *et al.*, 2018). After 5, 30 and 90 min, wounded thalli were harvested and immediately frozen and ground in liquid nitrogen. Four replicates of each genotype and time point were collected. Endogenous *cis*-OPDA, dn-*cis*-OPDA, dn-*iso*-OPDA, tn-*cis*-OPDA and tn-*iso*-OPDA were analysed using high-performance liquid chromatography electrospray-high-resolution accurate MS (HPLC-ESI-HRMS). For hormone extraction and purification, ± 100 mg of frozen powder was homogenized with 1 ml precooled (−20°C) methanol : water : HCOOH (90 : 9 : 1, v/v/v with 2.5 mM Na-diethyldithiocarbamate) and 10 µl of a stock solution of 1000 ng ml^{-1} of the deuterium-labelled internal standards [^{2}H$_5$]dnOPDA and [^{2}H$_5$]OPDA in methanol. Samples were extracted by shaking in a Multi Reax shaker (Heidolph Instruments, Schwabach, Germany) (60 min at 2000 rpm at room temperature). After extraction, solids were separated by centrifugation (10 min at 20 000 *g* at room temperature) in a Sigma 4-16K Centrifuge (Sigma Laborzentrifugen, Osterode am Harz, Germany), and re-extracted with an additional 0.5 ml extraction mixture, followed by shaking (20 min) and centrifugation. A quantity of 1 ml of the pooled supernatants was separated and evaporated at 40°C in a RapidVap Evaporator (Labconco Co., Kansas City, MO, USA). The residue was redissolved in 250 µl methanol/0.133% acetic acid (40 : 60, v/v) and centrifuged (10 min, 20 000 RCF, room temperature) before injection into the HPLC-ESI-HRMS system. Hormones were quantified using a Dionex Ultimate 3000 UHPLC device coupled to a Q Exactive Focus Mass Spectrometer (Thermo Fisher Scientific, Waltham, MA, USA) equipped with an HESI(II) source, a quadrupole mass filter, a C-trap, an higher energy collision-induced dissociation collision cell and an Orbitrap mass analyser, using a reverse-phase column (Synergi 4 mm Hydro-RP 80A, 150 × 2 mm; Phenomenex, Torrance, CA, USA). A linear gradient of methanol (A), water (B) and 2% acetic acid in water (C) was used: 38% A for 3 min, 38–96% A for 12 min, 96% A for 2 min, and 96–38% A for 1 min, followed by stabilization for 4 min. The percentage of C remained constant at 4%. The flow rate was 0.30 ml min^{-1}, the injection volume was 40 µl, and column and sample temperatures were 35 and 15°C, respectively. Standards of OPDA and [^{2}H$_5$]OPDA were purchased from OlChemim Ltd (Olomouc, Czech Republic), and standards of dn-OPDA and [^{2}H$_5$]dnOPDA were purchased from Cayman Chemical Co. (Ann Arbor, MI, USA). dn-*iso*-OPDA and tn-*iso*-OPDA were synthesized as previously described (Chini *et al.*, 2018; Monte *et al.*, 2018).

For FA measurements, samples of 3-wk-old plants were collected, freeze-dried and extracted (*c.* 10 mg, exact mass was recorded) and analysed as previously described (Ichihara & Fukubayasi, 2010). Nonadecanoic acid was used as the internal standard. GC-MS analysis was performed in an Agilent QTOF-A 7890B GC System (Santa Clara, CA, USA) coupled to a 7250 Accurate Mass Q-TOF and a 7693A Autosampler. The temperature program is as follows: the injection volume was 0.5 µl in an Agilent GC column DB5-MS (30 m long, ID 0.25 mm, and 0.25 µm film of 95% dimethyl/5% diphenylpolysiloxane) with a precolumn (10 m J&W integrated with Agilent 122-5532G) used for compound separation. Carrier gas flow rate (He) was set at 1.9852 ml min^{-1} and the split/splitless injector and transfer line temperatures were 250 and 280°C, respectively, and the split

ratio was 1 : 5. The initial column oven temperature was set at 80°C (held for 1 min), raised to 200°C at 15°C min^{-1}, to 280°C at 10°C min^{-1}, to 325°C at 25°C min^{-1} and held at this temperature for 7 min before cooling down for the next injection. The total run time was 25.8 min. The MS detection was performed with electron impact ionization (EI) at -70 eV of energy and 250°C in filament source (Table S2).

Gene expression analysis

A custom Marchantia microarray was used for WT and Mp*fad5* mutant lines (see Monte *et al.*, 2018). Three-week-old thalli were wounded with tweezers, collected after 90 min and their RNA extracted with FavorPrep Plant Total RNA Mini Kit (Vienna, Austria). Contaminating DNA was removed by DNase on-column digestion and sample quality was tested in a Bioanalyzer 2100 (Agilent Technologies, Santa Clara, CA, USA). Four independent biological replicates of wounded WT and Mp*fad5* plants were processed. Hybridizations, slide scanning and bioinformatic processing were performed as in Monte *et al.* (2018). Differentially expressed genes were selected by log-ratio values > 1 and < -1 and with an expected false discovery rate (FDR) (Limma) < 5%. Clustering of genes was performed using K-means with Euclidean distance (Soukas *et al.*, 2000) in Multi Experiment Viewer (http://mev.tm4.org/).

For quantitative PCR (qPCR) analysis, plants were grown as described earlier and then mechanically wounded with tweezers, or not. Tissue was collected at 90 min after treatment (for MpLOX8 (Mp2g12220) and MpCLAV.SYNTH (Clavaminate synthase-like; Mp3g11070)) and after 1, 2 or 4 d (for MpPATATIN (Mp5g21760), MpDIRIGENT (Mp5g16510) and MpbHLH62 (Mp2g00890) (wounding or mock)) and transferred directly to liquid nitrogen. Total RNA was extracted with the Favorgen plant RNA extraction kit including DNase treatment. Expression of marker genes was analysed by qPCR using MpAPT (Mp3g25140) as a reference gene.

Herbivory assays

Plates with seven plants of the WT and Mp*coi1-2*, and Mp*fad5-3* mutants were grown as described earlier for 3 wk. After this period, they were transferred to soil for another 3 wk. Then, 10 first-instar larvae of *S. exigua* (Entocare, Wageningen, the Netherlands) were released in each pot with 6-wk-old plants. Five pots were used for each genotype. To keep the insects in the pot, they were covered with perforated plastic boxes. After 1 wk of feeding, larvae were collected and weighed on a precision balance. To avoid the possibility that the lower size of Mpfad5 plants could be a limiting factor, we grew these plants in excess and there was always enough tissue left after collecting the larvae.

Individual flavonoid measurements

Concentration of main flavonoids found in *M. polymorpha* were measured by ultraperformance liquid chromatography (UPLC) using a Waters Acquity UPLC system (Waters Co., Milford, MA,

USA), following Soriano *et al.* (2019). The UPLC system was coupled to a micrOTOF II high-resolution MS (Bruker Daltonics, Bremen, Germany) equipped with an Apollo II ESI/APCI multimode source and controlled by the Bruker Daltonics Data Analysis software. Standards of apigenin and luteolin (Sigma-Aldrich) were used to quantify the five compounds, apigenin 7-*O*-glucuronide, apigenin 7,4′-di-*O*-glucuronide, luteolin 3′-*O*-glucuronide, luteolin 7′-*O*-glucuronide and luteolin 7,3′-di-*O*-glucuronide.

Statistical analysis

After checking the normality and homoscedasticity of the data (Shapiro–Wilk and Levene tests, respectively), the genotype (Figs 1, 3, 5a; see later) and/or treatment (Fig. 5b; see later) effect was tested for each variable using one-way ANOVA. When this test showed significant differences, means were then compared using Tukey's test. Different letters refer to statistically significant differences (Tukey's test). All the statistical procedures were performed with SPSS for Windows (SPSS Inc., Chicago, IL, USA).

Results

Identification of AtFAD5 orthologue in *Marchantia*

To determine if HTA (16:3n3) is a source of dn-OPDA in *Marchantia*, we first analysed the conservation of *FAD5*-related sequences in its genome. BLASTP sequence alignment and phylogenetic analysis revealed a single putative orthologue of At*FAD5* in *Marchantia*, corresponding to the gene *Mp3g10660*, which we subsequently named Mp*FAD5* (Fig. S2). To functionally characterize this gene, we generated loss-of-function mutants in the WT (Tak-1) background using CRISPR-Cas9 Nickase technology (Fauser *et al.*, 2014; Sugano *et al.*, 2018). Two independent mutant lines, Mp*fad5-3* and Mp*fad5-8*, were selected for experimentation. Both lines lacked the first exon, including 80 bp upstream the starting ATG, and Mp*fad5-3* also lacked the first 30 bp of the second exon (Figs 1a, S3). Preliminary phenotypic observation of these mutants suggested an alteration of growth and paler green pigmentation. Indeed, deeper analysis revealed retarded growth compared with the WT (Fig. 1b). Analysis of photosynthetic pigments indicated a reduced amount of total Chl in Mp*fad5* mutants (Fig. 1d), which is consistent with the phenotype of At*fad5* mutants (Heilmann *et al.*, 2004a). Moreover, measurement of F_v/F_m (variable/maximum fluorescence of PSII; an indicator of the state of the photosystem) demonstrated a reduction in PSII photochemical efficiency in Mp*fad5* plants, indicative of a stressed or perturbed photosynthetic apparatus (Fig. 1c). Mp*fad5* mutant plants also displayed a delay in antheridia formation after far red light (FR)-mediated induction (Fig. 1d–f). In some cases, plants did not generate sexual structures until 1 month after the WT, and in others the antheridia initially appeared brownish and finally aborted.

Mp*fad5* mutants display defects in the chloroplast structure

The lower PSII efficiency and the reduced growth rate of Mp*fad5* mutants suggested that they may have defective chloroplast
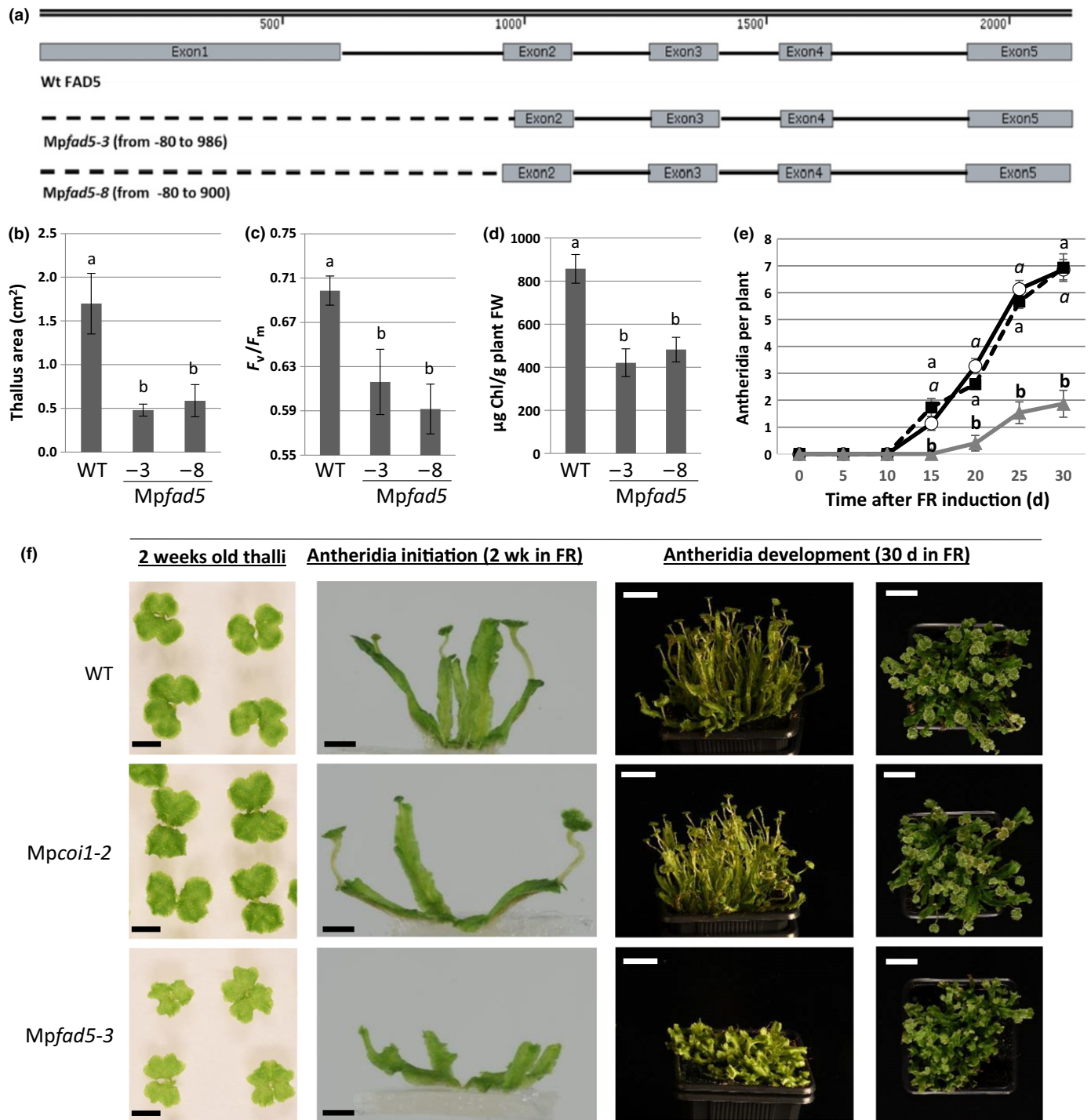
Fig. 1 Mp*fad5* phenotype. (a) Scheme of MpFAD5 gene of *Marchantia polymorpha*. Grey blocks represent exons, and dashed lines represent Mp*fad5* line deletions. (b–d) Thallus area (b), F_v/F_m measured in dark-adapted plants (c), and total chlorophyll (Chl) content g^{-1} plant FW (d) after 3 wk on culture. Four biological replicates were used for each analysis. (e) Timeline of number of antheridia per plant after far red (FR) induction (wild-type (WT), black line, squares, normal letter; Mp*coi1-2*, dashed black line, white circles and italics; Mp*fad5-3*, grey line, triangles and bold letters). (f) WT, Mp*coi1-2* and Mp*fad5-3* plants growing for 2 wk under constant light (first column, bars (black), 1 cm) and after 15 d supplemented with FR (second column, bars (black), 1 cm). Frontal and upper views of 2-month-old plants after 30 d of FR light supplementation (third and last columns, respectively; bars (white), 2 cm). Data shown in (b–f) are means ± SD (*n* = 4). For each variable, different letters showed significant differences between genotypes (one-way ANOVA with at least *P* < 0.05 + Tukey's test).

function. Electron microscopy images of Mp*fad5* chloroplasts (compared with the WT) revealed that their shape and internal organization were affected by the mutation. Although no differences were found in the total number or size of chloroplasts (Table S1), the mutants had aberrant chloroplasts with a range of different shapes, from very narrow structures to some that were

practically circular. This represents a marked difference to the classical oval shape of WT chloroplasts (Fig. 2). The organization of thylakoid and grana also appeared to be compromised by the Mp*fad5* mutation. In the WT, clearly differentiated structures were observed forming parallel groups between themselves and the cell membrane. In Mp*fad5* cells, however, the thylakoid and grana conformation was disorganized, losing its parallel conformation and showing curved and thickened parts throughout its structure. We also found numerous cytoplasmic invaginations (Fig. 2). These results indicate that FAD5 activity is essential for proper chloroplast development and function.

FAD5 is responsible for the synthesis of 16C PUFA and also affects the production of longer FAs

To establish whether the *FAD5* mutation affects the content of the main saturated and unsaturated FAs in *Marchantia*, we quantified prominent C16, C18 and C20 FAs in Mp*fad5* and WT plants by GC-MS (Table S2). Mp*fad5* alleles were mainly impaired in the accumulation of unsaturated C16 FAs (Fig. 3a). Neither HDA (16:2n6) nor HTA (16:3n3) were detected in Mp*fad5* alleles. A large reduction (70–80%; Fig. 3a) of the peak corresponding to $\sum$16:1s was also observed. This peak is composed of two different 16:1 FAs that coelute: 7*Z*-hexadecenoic (HD; 16:1n9) and palmitoleic acid (16:1n7) (Kramer *et al.*, 2002). As FAD5 is a Δ^7 desaturase (Heilmann *et al.*, 2004a) and the subproducts (HDA and HTA) of HD (16:1n9) were not detected, the reduction in this peak suggests the absence of HD, and the small observed amount of 16:1 should consist of palmitoleic acid (16:1n7). The contents of ALA (18:3n3) and eicosapentaenoic acid (EPA; 20:5n3) were also affected by the *FAD5* mutation (Figs 3b, S4). Mp*fad5* plants displayed a reduction of

around 40–50% for ALA and 25% for EPA compared with WT values. Altogether, these results indicate that MpFAD5 is responsible for the conversion of palmitic acid (16:0) into unsaturated C16:1n9 FA, which may contribute, at least partially, to the synthesis of longer FAs such as ALA and EPA.

Hexadecatrienoic acid is the main source of dn-OPDA in *M. polymorpha*

To assess how changes in FA composition in Mp*fad5* affect the content of jasmonate-related oxylipins in *Marchantia*, we evaluated the accumulation pattern of these molecules after mechanical wounding in a time course experiment (Fig. 3c). Significant differences were found between WT and Mp*fad5* lines for all measured jasmonates. Concentrations of both OPDA and tn-OPDA were seen to be moderately reduced, compared with the WT. This finding was consistent with the reduction of ALA (18:3n3) in the Mp*fad5* mutant lines. The greatest differences, however, were observed in dn-*cis*- and dn-*iso*-OPDA contents. In Mp*fad5* mutants, dn-*iso*-OPDA concentrations reached only *c.* 5% of that observed in WT plants, while dn-*cis*-OPDA was almost absent (< 1%) in the mutant samples.

The strong reduction in dn-OPDA isomers correlate with the strong reduction in C16 FAs, whereas the reduction in OPDA, not significant at 30 min, but over 50% of the wound-induced concentrations at 5 and 90 min, correlates with the smaller reduction in ALA (18:3n3). Taken together, these results indicate that HTA (16:3n3) is the main source of both dn-OPDA isomers in *Marchantia*, contributing to *c.* 95% of the total content (*c.* basal, 1%; 5 min, 3%; 30 min, 10%; and 90 min, 8%). The contribution of OPDA to dn-OPDA production is, however, secondary and, at most, 5%. In addition, the higher accumulation of
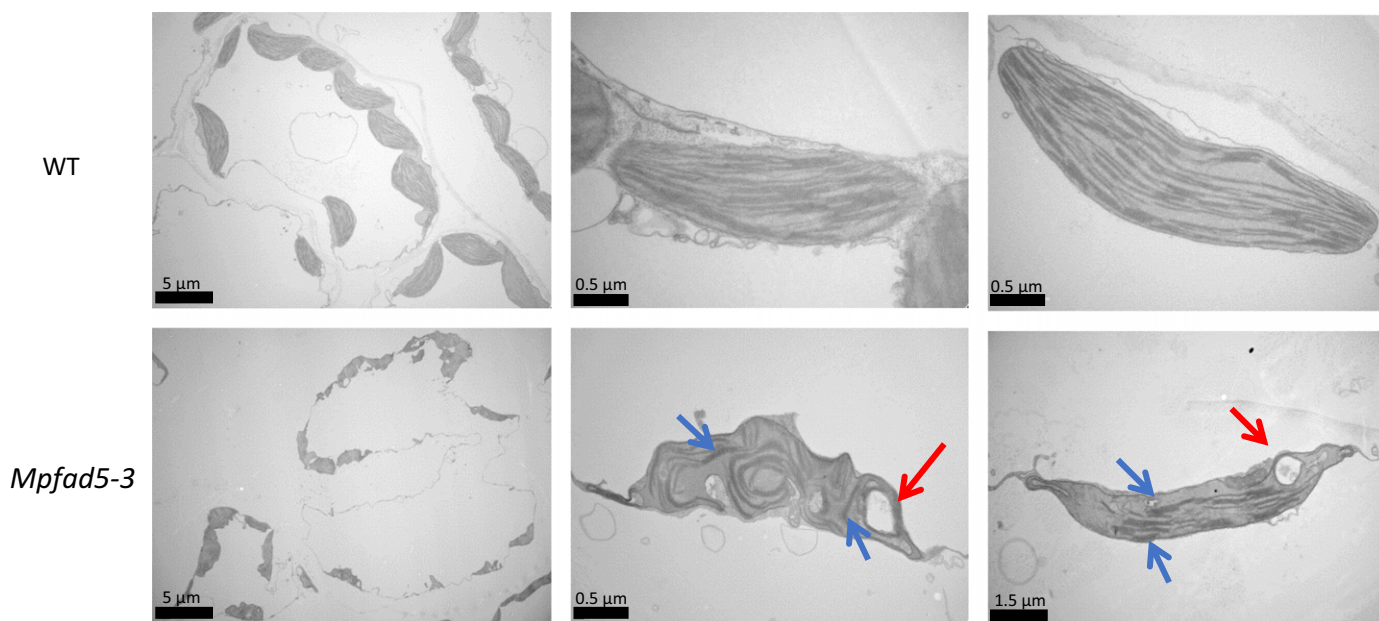

Fig. 2 Chloroplast microscopy analysis. Electronic microscopy images of *Marchantia polymorpha* wild-type (WT) and Mp*fad5-3* cells from the photosynthetic region of thallus (bar, 5 μm (first column)). Detail of WT and Mp*fad5-3* single chloroplasts (bars: 0.5 μm (second and third columns); 1.5 μm (last column of Mp*fad5-3*)). Blue arrows indicate compressed grana. The red arrow indicates cytoplasm invagination.
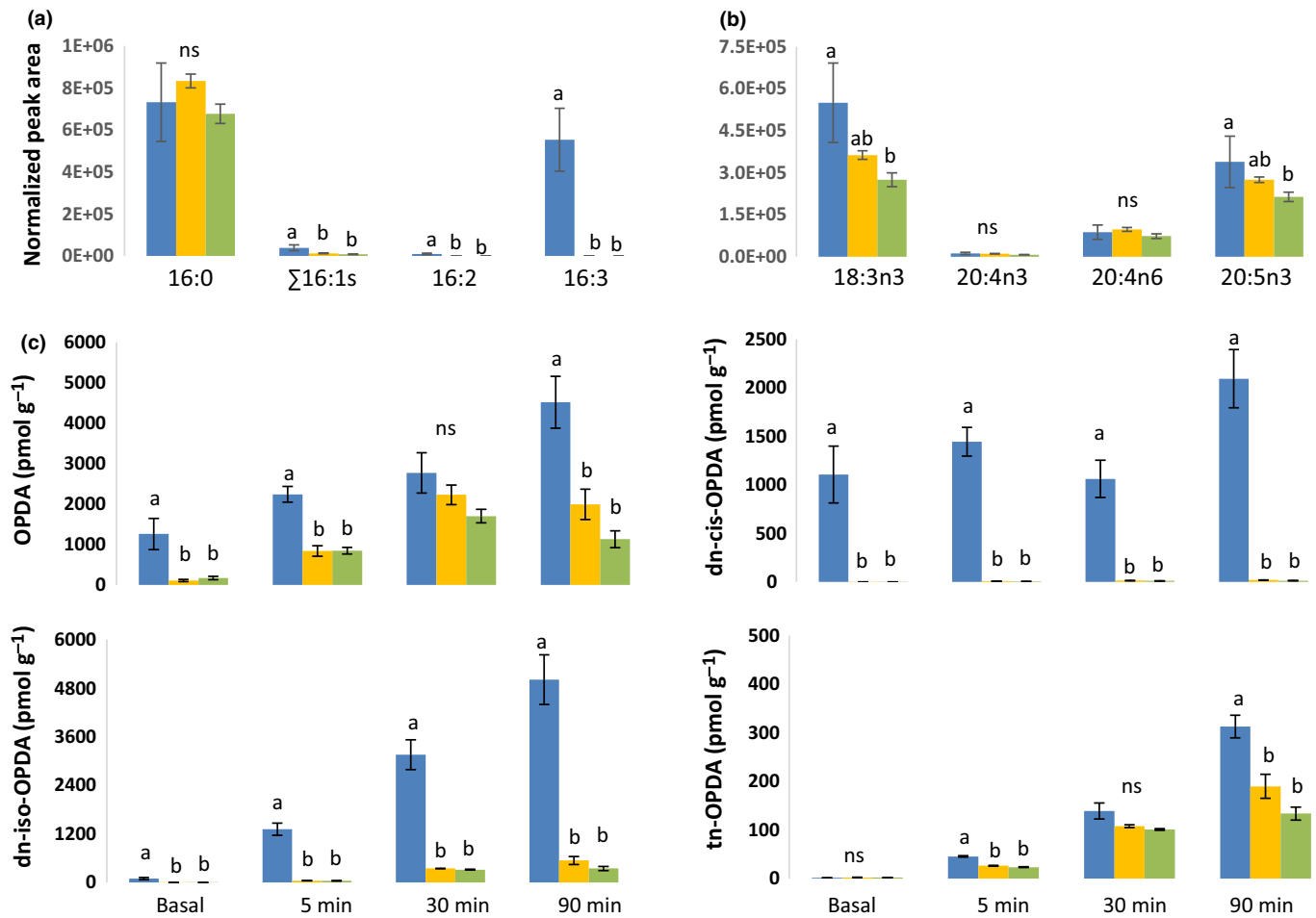
Fig. 3 Fatty acid and jasmonate measurements in *Marchantia polymorpha*. (a, b) Content of C16 fatty acids (16:0 (palmitic acid), ∑ 16:1s (16:1Δ7 (7Z-hexadecenoic acid) + 16:1Δ9 (palmitoleic acid)), 16:2 (hexadecadienoic acid (HAD)) and 16:3 (hexadecatrienoic acid (HTA)) (a) and some C18 and C20 fatty acids, 18:3n3 (α-linolenic acid (ALA)), 20:4n3 (eicosatetraenoic acid (ETA)), 20:4n6 (arachidonic acid (ARA)) and 20:5n3 (eicosapentanoic acid (EPA)) (b) in wild-type (WT) (blue bars) and Mp*fad5* lines (−3, yellow; −8, green bars). (c) Time-course accumulation of 12-oxo-phytodienoic acid (OPDA), dinor-*cis*-OPDA (dn-*cis*-OPDA), dn-*iso*-OPDA and tetranor-OPDA (tn-OPDA) in WT (blue bars) and both Mp*fad5* mutant lines (−3, yellow; and −8, green bars) in basal conditions and 5, 30 and 90 min after mechanical wounding. Data are means ± SD ($n = 4$). For each variable, different letters show significant differences between genotypes (one-way ANOVA $P < 0.05$ + Tukey's test).

dn-*iso*-OPDA (compared with dn-*cis*-) in the mutant suggests that the kinetics of dn-*cis*- to dn-*iso*-OPDA conversion is faster than both the synthesis of dn-*cis*-OPDA from 16:3 and the β-oxidation of dn-*cis*-OPDA to produce tn-OPDA.

dn-OPDA-mediated gene expression is only partially compromised in Mp*fad5*

Responses to mechanical wounding and insect feeding are among the main responses regulated by dn-OPDA isomers in *Marchantia* (Monte *et al.*, 2018). To evaluate whether the reduction of dn-*cis/iso*-OPDA concentrations in Mp*fad5* alleles impairs responses to wounding, we obtained transcriptomic profiles of wounded *Marchantia* mutants and compared them with those of wounded WT plants. A total of 297 genes were differentially expressed (DE) by wounding in Mp*fad5* compared with WT plants (log ratio > |1|, FDR < 0.05). Clustering and gene ontology (GO) analyses comparing Mp*fad5* DE genes with previous

data obtained in our laboratory (WT response to wounding, to OPDA treatment and DE genes in Mp*coi1* mutants in response to OPDA) revealed that most DE genes upregulated in Mp*fad5* were involved in chloroplast development and function, including responses to light (Clusters 4 and 5; Fig. 4a,b). These results are consistent with the phenotypic defects in chloroplasts, Chl content and PSII efficiency in Mp*fad5* alleles (Fig. 2).

Further to this, our analyses identified a group of the downregulated genes in Mp*fad5* to be genes regulated by wounding, OPDA or MpCOI1 (clusters 1 and 2; Fig. 4a). The top section of cluster 1 represents genes regulated by wounding, OPDA and MpCOI1, whereas the bottom part represents genes regulated by wounding and OPDA, but independent of MpCOI1. Cluster 2 represents genes regulated by MpCOI1 but not by wounding or OPDA. Gene ontology and qPCR analyses confirmed our data. The GO term 'response to wounding' was enriched in cluster 1, whereas 'response to other organisms' was enriched in cluster 2 (Fig. 3b; lanes 1 and 2). The qPCR analysis of early and late
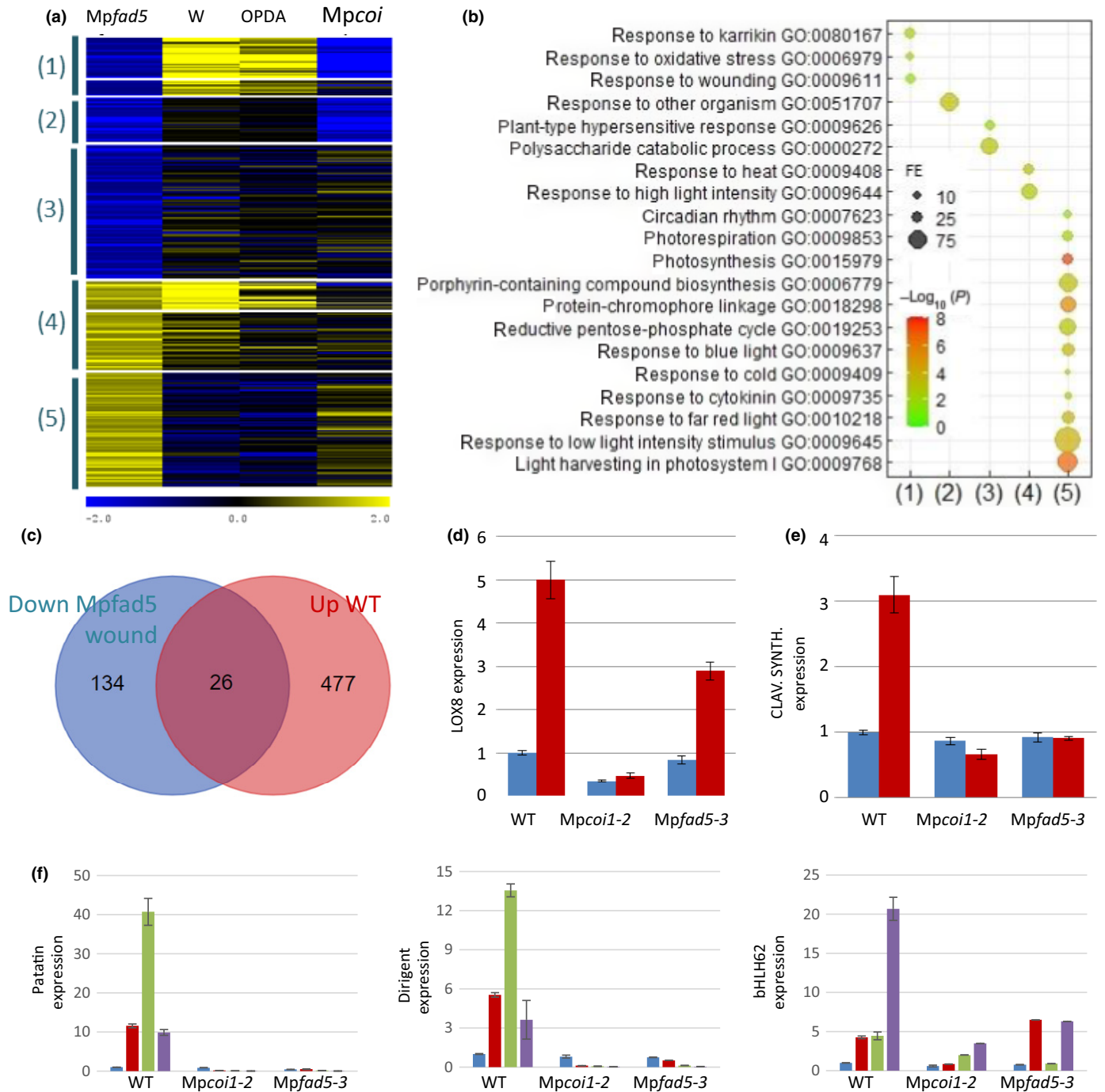
Fig. 4 Gene expression analysis in *Marchantia polymorpha* after wounding. (a) K-means clustering of genes differentially expressed in response to wounding or 12-oxo-phytodienoic acid (OPDA) in different genotypes. Mp*fad5*, Mp*fad5* wound vs wild-type (WT) wound; W, WT wound vs WT mock; OPDA, WT OPDA vs WT mock; mp*coi1*, mp*coi1* OPDA vs WT OPDA. Differentially expressed genes were selected from the Mp*fad5* experiment ($\log_2$(Mp*fad5*/WT) > |1|, FDR < 0.05), and their expression in the rest of the genotypes and treatments were obtained from available data. Seven clusters were generated and some pairs with similar patterns were grouped for gene ontology (GO) analyisis (numbers in brackets). (b) Significant GO terms (biological process) associated with each of the groups in (b). FE, fold-enrichment of the term in the cluster. GO terms correspond to the most similar genes in Arabidopsis. (c) Overlapping of genes downregulated in Mp*fad5* and upregulated in the WT in response to wounding. Differentially expressed genes were selected as in (a). (d, e) Quantitative PCR (qPCR) analysis of two COI-dependent wound-induced marker genes in basal conditions (blue bars) and at 90 min after wounding (red bars). (f) qPCR analysis of three COI-dependent wound-induced marker genes in basal conditions (blue bars) and at 1, 2 or 4 d after wounding (red, green and purple bars, respectively). In both qPCR analyses, gene expression was normalized against MpAPT. Error bars represent SD ($n = 3$).

dn-OPDA-responsive marker genes (Mp*PATATIN*, Mp*DIRIGENT*, Mp*bHLH62*, Mp*LOX8* and Mp3g11070 (*Clavaminate synthase-like*)) showed marked differences in wound-mediated induction between the WT and Mp*fad5*, consistent with the wound/OPDA regulation of genes in both clusters 1 and 2, and further supported the possibility that genes in cluster 2 might represent late wound-responsive genes (Fig. 4c). These results support the importance of dn-OPDA and MpFAD5 in the MpCOI1-dependent response to wounding. A subset of OPDA-responsive COI1-independent genes was observed to be activated by wounding in the Mp*fad5* plants, and these can probably be attributed to the remaining OPDA concentrations found in the mutants (Fig. 3c, cluster 4; Fig. 4a). OPDA is known to regulate some genes through its electrophilic properties, independently of COI1, and consistent with recent findings, the COI1-independent genes that were unaffected in the Mp*fad5* mutant were associated with the GO term 'response to heat' (Fig. 4b, lane 4; Monte *et al.*, 2020). The fact that these genes are also associated with the GO term 'response to high light' is consistent with their overexpression in the 'chloroplast-stressed' Mp*fad5* mutants.

Surprisingly, however, when considering the huge number of genes regulated by wounding in WT plants (Fig. 4c), the relative contribution of MpFAD5 to COI1-dependent wound-related responses was much lower than we expected. Indeed, among the 503 genes induced by wounding in WT plants, only 26 were DE in Mp*fad5* plants. This result is probably influenced by the small quantity of dn-*iso*-OPDA accumulating in Mp*fad5* (Fig. 3c). However, given that *c.* 95% of normal dn-*iso*-OPDA concentrations are lost in this mutant, these data could also suggest that dn-OPDA is not the only molecule activating the wound response in *Marchantia*.

Mp*fad5* plants have a WT-like response to herbivory

To further study the consequence of reduced dn-OPDA isomers and the role of MpFAD5 in defence, Mp*fad5* mutants were subjected to herbivory using WT and Mp*coi1-2* plants as control. First-instar larvae of the generalist herbivore *Spodoptera exigua* were released on 6-wk-old *Marchantia* plants and their

performance (larval weight) was measured after 7 d. In agreement with previous results (Monte *et al.*, 2018), larvae fed on Mp*coi1-2* were significantly larger than those collected from WT plants (Fig. 5a). However, and despite the extremely low concentrations of dn-OPDA, those fed on Mp*fad5* plants were not significantly different from those fed on WT plants, indicating that defences against herbivores are not impaired in Mp*fad5*.

As light stress induces flavonoid accumulation in *Marchantia* (Albert *et al.*, 2018; Soriano *et al.*, 2019) and flavonoids are known to be involved in defence against herbivores (Morimoto *et al.*, 2000; Qi *et al.*, 2008), we analysed the flavonoid contents in Mp*fad5* after herbivory employing an experimental setup similar to that in Fig. 5(a) (7 d after treatment). *Marchantia* has previously been shown to accumulate mainly apigenin- and luteolin-derived flavones (Markham & Porter, 1974; Soriano *et al.*, 2019, 2021). As shown in Fig. 5(b), Mp*fad5* mutants accumulated higher levels than the WT for all measured flavonoids in basal conditions. Similarly, after herbivory, Mp*fad5* showed higher values of apigenin derivatives (apigenin 7-*O*-glucuronide and apigenin 7,4′-di-*O*-glucuronide) and also for one luteolin (luteolin 7′-*O*-glucuronide), in comparison to WT plants.

These results show that despite severe reduction in dn-OPDA concentrations in the absence of MpFAD5, the plant defences are unaffected. Given that only minor perturbations of the wound responses were seen, taken together our data indicate that dn-OPDA may be able to activate a near-normal jasmonate response even when limited to only 5% of the usual post-wounding concentration. Alternatively, our data firmly raise the possibility of an alternate signalling molecule that may act redundantly with dn-OPDA in the activation of jasmonate responses.

Discussion

Despite the importance of dn-OPDA as the bioactive jasmonate (i.e. the COI1 ligand in *Marchantia*), details of its biosynthesis in bryophytes are still unclear. Previous work in *Arabidopsis* suggested two possible routes for dn-OPDA production: the hexadecanoid pathway, producing dn-OPDA directly from HTA (16:3n-3), and the octadecanoid pathway, producing the molecule indirectly from ALA (18:3n3, via an
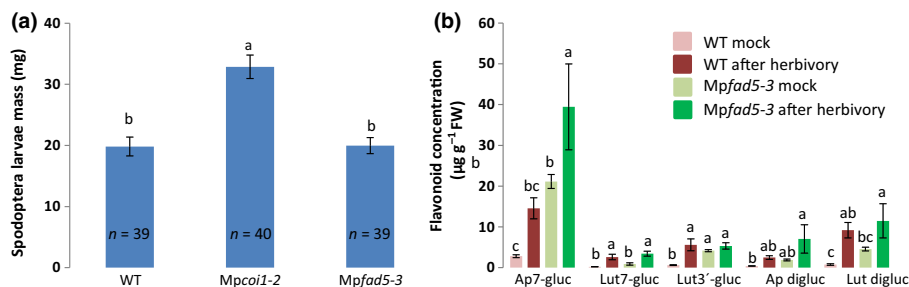

Fig. 5 Larval infection. (a) *Spodoptera exigua* larval weight after 7 d feeding on *Marchantia polymorpha* thalli of wild-type (WT) and Mp*coi1-2* and Mp*fad5-3* mutants. (b) Content of main flavonoids found in *M. polymorpha* (WT, reddish bars; Mp*fad5-3*, green bars) in mock (paler bars) and after herbivory stress (darker bars). Ap7-gluc, apigenin 7-*O*-glucuronide; Lut7-gluc, luteolin 7-*O*-glucuronide; Lut3′-gluc, luteolin 3′-*O*-glucuronide; Ap digluc, apigenin 7,4′-di-*O*-glucuronide; Lut digluc, luteolin 7,3′-di-*O*-glucuronide. Data are means ± SE (a) and means ± SD in (*n* = 3) (b). For each variable, different letters show significant differences between genotypes and/or treatments (one-way ANOVA, *P* < 0.05 + Tukey's test).

OPR3-independent conversion of OPDA to dn-OPDA (Weber *et al.*, 1997; Chini *et al.*, 2018)). In *Marchantia*, exogenous treatment with labelled ALA (18:3n3) and HTA (16:3n3) confirmed that both FAs are potential dn-OPDA precursors (Monte *et al.*, 2018), although their relevance *in vivo* was not addressed. Here, by analysing Mp*fad5* mutants, we show that although some conversion of OPDA into dn-OPDA is possible, particularly after exogenous treatment, the main source of dn-OPDA in *Marchantia* is the hexadecanoid pathway (i.e. HTA (16:3n-3)), and the contribution of the octadecanoid pathway is minimal. Moreover, we show the functional conservation of FAD5 in species separated by more than 450 million yr of independent evolution, suggesting that this function evolved in the common ancestor of all land plants.

Similar to At*fad5* (Heilmann *et al.*, 2004a), Mp*fad5* mutants lack Δ^7-desaturase function and, therefore, are not able to synthesize HD (16:1n9), HAD (16:2n6) and HTA (16:3n3). By contrast, 18:1 and 18:2 levels are unaffected and 18:3 levels remain high in Mp*fad5*. The consequence of blocking the hexadecanoid pathway in Mp*fad5* is a reduction of *c.* 95% of the dn-OPDA content and virtually 100% of the dn-*cis*-OPDA isomer. Thus, the octadecanoid pathway, and the conversion of OPDA into dn-OPDA, is clearly a secondary and minor source for the synthesis of this compound, accounting for, at most, 5% of the total dn-OPDA content *in vivo*.

Blockage of the hexadecanoid pathway in Mp*fad5* is characterized by the absence of 16:2 and 16:3 in this mutant. However, MpFAD5 catalyses the unsaturation of 16:0 to 16:1 and the peak corresponding to 16:1 does not fully disappear in the mutants. This peak is composed of two different 16:1 FAs that coelute: 7*Z*-hexadecenoic (HD; 16:1n9) and palmitoleic acid (16:1n7) (Kramer *et al.*, 2002). As FAD5 is a Δ^7-desaturase (Heilmann *et al.*, 2004a) and the subproducts (HDA and HTA) of HD (16:1n9) were not detected, the presence of this peak can be attributed to palmitoleic acid, with the reduction in the peak size being caused by the absence of HD. *Marchantia* has three different orthologues of *Arabidopsis* FAB-family member FAB2, one of which displays high similarity to a Δ^9-desaturase involved in palmitic acid synthesis in the diatom *Phaeodactylum tricornutum* (Liu *et al.*, 2020). The remaining content of palmitoleic acid (16:1) could therefore be explained by the actions of this MpFAB2.

Despite the functional conservation between AtFAD5 and MpFAD5, differences in FA profile between Mp*fad5* and WT plants suggest that FAD5 function in *Marchantia* may be more extensive than in *Arabidopsis*. While 16C FAs in At*fad5* mutants are clearly reduced, 18C FAs were found to be unaffected (Heilmann *et al.*, 2004a). By contrast, our data demonstrate that in Mp*fad5*, 18:3n3 levels are lower than in WT, as are levels of the longer chain FA, 20:5n3 (which is not present in *Arabidopsis*). The wider-reaching effects of MpFAD5 on longer-chain FAs may be explained by divergences in FAD5 function between *Arabidopsis* and *Marchantia*, changes that have probably resulted from differences in the relative contribution of other proteins involved in FA biosynthesis. Indeed, one of the main differences between the genomes of these two species is the degree of gene

redundancy, which is much greater in *Arabidopsis* than in *Marchantia*. In this instance, this is hugely relevant as the ADS (*Arabidopsis* desaturase) family, which is numerous in *Arabidopsis* (including eight ADSs besides AtFAD5), is greatly diminished in *Marchantia*, which has only one ADS member, MpFAD5 (Fig. S2). Previous studies on AtADSs have shown that their regiospecificity varies according to their intracellular location (i.e. they act as Δ^7 in the plastids and as Δ^9 in the cytoplasm) and that consequently they can desaturate not only palmitic acid but also stearic acid (Heilmann *et al.*, 2004b). Thus, being the only member of the ADS family in *Marchantia*, MpFAD5 may integrate several of the functions distributed across distinct genes in *Arabidopsis* and consequently can participate in the desaturation of both types of FAs (C16 and C18). As such, it appears that a significant part of the evolution of the ADS family in *Arabidopsis* has involved functional specialization. Alternatively, HTA can be elongated to ALA in certain fungi and algae, such as *Penicillium chrysogenum* or *Cyanidium caldarium* (Richards & Quackenbush, 1974; Bedord *et al.*, 1978). Whether this HTA to ALA elongation can occur also in *Marchantia* or in other land plants needs to be explored.

The analysis of Mp*fad5* mutants also uncovered that the deficit in unsaturated 16C FAs significantly affects the shape and function of chloroplasts. In addition to changes in chloroplast morphology, other markers of the chloroplasts being in poor condition included compressed grana and the presence of unusual invaginations (Woodson, 2019; Alamdari *et al.*, 2021; Lemke *et al.*, 2021). This defect in the structure of chloroplast membranes results in a poor performance of the photosynthetic apparatus. F_v/F_m values of Mp*fad5* mutant plants indicate that these plants were stressed (photoinhibited) in basal growth conditions. Previous studies in *Marchantia* have shown that F_v/F_m values depend on light conditions, with lower values (photoinhibited) at high radiation (Soriano *et al.*, 2019). Gene expression analysis confirmed a constitutive response to light stress, a likely consequence of the defects in chloroplast development.

Developmental defects in the photosynthetic apparatus resulted in a lower growth rate, a pale green phenotype and other anomalous light responses such as the delay in archegonia formation (regulated by FR light; Inoue *et al.*, 2019). Notably, the pale green phenotype is also characteristic of the At*fad5* mutant in *Arabidopsis* and the tomato *spr2* mutant, which cannot synthesize HTA (Li *et al.*, 2003; Heilmann *et al.*, 2004a). Hexadecatrienoic acid (16:3n3) is one of the main components of monogalactosyl-diacylglycerols (MGDGs) in the so-called 16:3 plants (those with a predominance of the prokaryotic route, such as *Arabidopsis* and *Marchantia*; Reszczyńska & Hanaka, 2020). These, together with digalactosyl-diacylglicerols (DGDGs), containing mainly 18:3 FAs, are the predominant lipids found in thylakoid membranes. Although chloroplast development has not been analysed in At*fad5* or Sl*spr2*, the phenotypic coincidence in these evolutionary distant species strongly suggests that HTA (16:3n3) is essential for chloroplast membrane integrity and organelle development in 16:3 plants.

Besides a strong activation of chloroplasts and light stress-related genes in Mp*fad5*, our transcriptomic analyses revealed a

defect in the induction of a subset of dn-OPDA regulated genes, which are activated by MpCOI1 and the jasmonate pathway in response to wounding. Although these data support a role for MpFAD5 and HTA (16:3n3) in dn-OPDA biosynthesis and signalling, it was surprising to observe that the deficit in the transcriptional response to mechanical wounding was not much greater. Given the extent to which dn-OPDA concentrations are reduced in Mp*fad5* mutant plants, it is somewhat remarkable that the majority of the wound-responsive genes were unaffected in this line. One possibility is that the wound-related gene activation is indeed a result of the small quantity of dn-*iso*-OPDA accumulating in Mp*fad5*. Bioactive jasmonates tend to 'saturate' at much lower concentrations than their precursors, but it is unknown what concentration of the hormone is actually required to trigger a complete (or indeed, a partial) response. The data presented here indicate that the plant is accumulating a much higher level of the COI1-ligand than is needed and only very low levels are sufficient to regulate large branches of the signalling pathway.

In addition to many wound-responsive genes being unaffected in Mp*fad5* plants, a subset of dn-OPDA regulated heat response genes were found to be upregulated. Heat stress genes are specifically regulated by dn-*cis*-OPDA (and not by dn-*iso*-OPDA, which lacks electrophilic properties; Monte *et al.*, 2020). The Mp*fad5* mutant accumulates a reduced but still considerable concentration of OPDA. Like dn-*cis*-OPDA, OPDA has an α,β-unsaturated carbonyl group which confers electrophilic properties (Monte *et al.*, 2020) and thus the OPDA may be responsible for the activation of these genes in a 'chloroplast stressed' Mp*fad5* mutant.

The *Arabidopsis* mutant *opr3* possesses similar concentrations of the vascular plant hormone, JA-Ile, to dn-OPDA in Mp*fad5* (i.e. *c.* 5%) (Chini *et al.*, 2018). However, At*opr3* plants showed an increased susceptibility to herbivorous insects compared with the WT, whereas Mp*fad5* displayed WT amounts of resistance. One explanation for this is the increased concentration of flavonoids, such as apigenin and luteolin derivatives, that are constitutively found in Mp*fad5* mutants. These flavonoids have been shown to have antifeedant activity (Golawska & Lukasik, 2012; El Shafeiy & Abdelaziz, 2020) and thus may have contributed to the protection of the mutant plants. Furthermore, it has been found that an adequate qualitative and quantitative composition of FAs in the diet is very important for optimal insects' development (Hoc *et al.*, 2020), and therefore the reduced concentrations of specific FAs in Mpfad5 may also contribute to the unexpectedly poor larval performance on these plants.

Despite this, the near-normal jasmonate-regulated transcriptomic response in Mp*fad5* mutants does suggest that the resistance to herbivory in these plants cannot be explained by flavonoid content and reduced ω3 VLPUFA levels alone. It is tempting to speculate that dn-OPDA is not the only jasmonate activating wound responses in *Marchantia*. Our data suggest the potential for an as-yet-undiscovered molecule(s) which may act synergistically with dn-OPDA to activate defence responses against both mechanical wounding and herbivory. *Marchantia*

membranes contain several VLPUFAs (Lu *et al.*, 2019), which are not common in vascular plants, and may act as a source for alternate signalling molecules in the jasmonate pathway. As the study of jasmonates in plants besides *Arabidopsis* has, until recently, been largely absent in the scientific literature, the contribution of VLPUFAs to jasmonate signalling has been greatly overlooked. Our findings thus indicate that new branches of the jasmonate pathway and clues to its evolution may be hidden within different plant species, presenting an exciting future challenge for the field.

Author contributions

GS, SK, GJ-A and RS conceptualized and designed the research. GS, SK and GJ-A conducted all experiments and analysed the data. AMZ, JMG-M, FR-SV and CB carried out all metabolite measurements. JMF-Z made transcriptomic analyses. GS, SK, GJ-A and RS wrote the manuscript with input from all co-authors. All authors reviewed and approved the manuscript.

ORCID

Coral Barbas https://orcid.org/0000-0003-4722-491X
José Manuel Franco-Zorrilla https://orcid.org/0000-0001-6769-7349
Jose M. García-Mina https://orcid.org/0000-0001-6352-9612
Guillermo Jimenez-Aleman https://orcid.org/0000-0002-6930-9589
Sophie Kneeshaw https://orcid.org/0000-0003-3966-9505
Mª Fernanda Rey-Stolle https://orcid.org/0000-0002-0873-4485
Roberto Solano https://orcid.org/0000-0001-5459-2417
Gonzalo Soriano https://orcid.org/0000-0002-1728-7656
Ángel M. Zamarreño https://orcid.org/0000-0003-1966-0239

Data availability

References

Aid F. 2019. Plant lipid metabolism. In: Valenzuela R, ed. *Advances in lipid metabolism*. London, UK: IntechOpen, 1–16.

Alamdari K, Fisher KE, Tano DW, Rai S, Palos K, Nelson ADL, Woodson JD. 2021. Chloroplast quality control pathways are dependent on plastid DNA synthesis and nucleotides provided by cytidine triphosphate synthase two. *New Phytologist* **231**: 1431–1448.

Albert NW, Thrimawithana AH, Mcghie TK, Clayton WA, Deroles SC, Schwinn KE, Bowman JL, Jordan BR, Davies KM. 2018. Genetic analysis of the liverwort *Marchantia polymorpha* reveals that *R2R3MYB* activation of flavonoid production in response to abiotic stress is an ancient character in land plants. *New Phytologist* **218**: 554–566.

Arondel V, Lemieux B, Hwang I, Gibson S, Goodman HM, Somerville CR. 1992. Map-based cloning of a gene controlling ω-3 fatty acid desaturation in *Arabidopsis*. *Science* **258**: 1353–1355.

Bedord CJ, McMahon V, Adams B. 1978. α-linolenic acid byosinthesis in *Cyanidium caldarium*. *Archives of Biochemistry and Biophysics* **185**: 15–20.

Browse J, Kunst L, Anderson S, Hugly S, Somerville C. 1989. A mutant of *Arabidopsis* deficient in the chloroplast 16:1/18:1 desaturase. *Plant Physiology* **90**: 522–529.

Chini A, Fonseca S, Fernández G, Adie B, Chico JM, Lorenzo O, García-Casado G, López-Vidriero I, Lozano FM, Ponce MR *et al.* 2007. The *JAZ* family of repressors is the missing link in jasmonate signalling. *Nature* **448**: 666–671.

Chini A, Gimenez-Ibanez S, Goossens A, Solano R. 2016. Redundancy and specificity in jasmonate signalling. *Current Opinion in Plant Biology* **33**: 147–156.

Chini A, Monte I, Zamarreño AM, Hamberg M, Lassueur S, Reymond P, Weiss S, Stintzi A, Schaller A, Porzel A *et al.* 2018. An *OPR3*-independent pathway uses 4,5-didehydrojasmonate for jasmonate synthesis. *Nature Chemical Biology* **14**: 171–178.

Chiyoda S, Ishizaki K, Kataoka H, Yamato KT, Kohchi T. 2008. Direct transformation of the liverwort *Marchantia polymorpha* L. by particle bombardment using immature thalli developing from spores. *Plant Cell Reports* **27**: 1467–1473.

El Shafeiy S, Abdelaziz S. 2020. Insects' deterrent flavonoids from *Cynara cardunculus* for controlling cotton leafworm, *Spodoptera littoralis*. *Journal of Plant Protection and Pathology* **11**: 315–320.

Farmer EE, Mueller MJ. 2013. ROS-mediated lipid peroxidation and RES-activated signaling. *Annual Review of Plant Biology* **64**: 429–450.

Fauser F, Schiml S, Puchta H. 2014. Both CRISPR/Cas-based nucleases and nickases can be used efficiently for genome engineering in *Arabidopsis thaliana*. *The Plant Journal* **79**: 348–359.

Fernández-Calvo P, Chini A, Fernández-Barbero G, Chico JM, Gimenez-Ibañez S, Geerinck J, Eeckhout D, Sweizer F, Godoy M, Franco-Zorrilla JM *et al.* 2011. The *Arabidopsis* bHLH transcription factors MYC3 and MYC4 are targets of JAZ repressors and act additively with MYC2 in the activation of jasmonate responses. *Plant Cell* **23**: 701–715.

Fonseca S, Chico JM, Solano R. 2009. The jasmonate pathway: the ligand, the receptor and the core signalling module. *Current Opinion in Plant Biology* **12**: 539–547.

Gibson S, Arondel V, Iba K, Somerville C. 1994. Cloning of a temperature-regulated gene encoding a chloroplast omega-3 desaturase from *Arabidopsis thaliana*. *Plant Physiology* **106**: 1615–1621.

Goławska S, Łukasik I. 2012. Antifeedant activity of luteolin and genistein against the pea aphid, *Acyrthosiphon pisum*. *Journal of Pest Science* **85**: 443.

He M, Qin C-X, Wang X, Ding N-Z. 2020. Plant unsaturated fatty acids: biosynthesis and regulation. *Frontiers in Plant Science* **11**: 390.

Heilmann I, Mekhedov S, King B, Browse J, Shanklin J. 2004a. Identification of the *Arabidopsis* palmitoyl-monogalactosyldiacylglycerol delta7-desaturase gene FAD5, and effects of plastidial retargeting of *Arabidopsis* desaturases on the fad5 mutant phenotype. *Plant Physiology* **136**: 4237–4245.

Heilmann I, Pidkowich MS, Girke T, Shanklin J. 2004b. Switching desaturase enzyme specificity by alternate subcellular targeting. *Proceedings of the National Academy of Sciences, USA* **101**: 10266–10271.

Hoc B, Genva M, Fauconnier ML, Lognay G, Francis F, Caparros-Megido R. 2020. About lipid metabolism in *Hermetia illucens* (L. 1758): on the origin of fatty acids in prepupae. *Scientific Reports* **10**: 11916.

Howe GA, Major IT, Koo AJ. 2018. Modularity in jasmonate signaling for multistress resilience. *Annual Review of Plant Biology* **69**: 387–415.

Ichihara K, Fukubayashi Y. 2010. Preparation of fatty acid methyl esters for gas-liquid chromatography. *Journal of Lipid Research* **51**: 635–640.

Inoue K, Nishihama R, Araki T, Kohchi T. 2019. Reproductive induction is a far-red high irradiance response that is mediated by phytochrome and PHYTOCHROME INTERACTING FACTOR in *Marchantia polymorpha*. *Plant and Cell Physiology* **60**: 1136–1145.

Katsir L, Schilmiller AL, Staswick PE, He SY, Howe GA. 2008. COI1 is a critical component of a receptor for jasmonate and the bacterial virulence factor coronatine. *Proceedings of the National Academy of Sciences, USA* **105**: 7100–7105.

Kramer JKG, Blackadar CB, Zhou J. 2002. Evaluation of two GC columns (60-m SUPELCOWAX 10 and 100-m CP Sil 88) for analysis of milkfat with emphasis on CLA, 18:1, 18:2 and 18:3 isomers, and short- and long-chain FA. *Lipids* **37**: 823–835.

Kubota A, Ishizaki K, Hosaka M, Kohchi T. 2013. Efficient *Agrobacterium*-mediated transformation of the liverwort *Marchantia polymorpha* using regenerating thalli. *Bioscience, Biotechnology, and Biochemistry* **77**: 167–172.

Kubota A, Kita S, Ishizaki K, Nishihama R, Yamato KT, Kohchi T. 2014. Co-option of a photoperiodic growth-phase transition system during land plant evolution. *Nature Communications* **5**: 1–9.

Lemke MD, Fisher KE, Kozlowska MA, Tano DW, Woodson JD. 2021. The core autophagy machinery is not required for chloroplast singlet oxygen-mediated cell death in the *Arabidopsis thaliana* plastid ferrochelatase two mutant. *BMC Plant Biology* **21**: 1–20.

Li C, Liu G, Xu C, Lee GI, Bauer P, Ling H-Q, Ganal MW, Howe GA. 2003. The tomato suppressor of prosystemin-mediated responses2 gene encodes a fatty acid desaturase required for the biosynthesis of jasmonic acid and the production of a systemic wound signal for defense gene expression. *Plant Cell* **15**: 1646.

Liu B, Sun Y, Hang W, Wang X, Xue J, Ma R, Jia X, Li R. 2020. Characterization of a novel acyl-ACP Δ^9 desaturase gene responsible for palmitoleic acid accumulation in a diatom *Phaeodactylum tricornutum*. *Frontiers in Microbiology* **11**: 584589.

Lorenzo O, Chico JM, Sanchez-Serrano JJ, Solano R. 2004. JASMONATE-INSENSITIVE1 encodes a MYC transcription factor essential to discriminate between different jasmonate-regulated defense responses in *Arabidopsis*. *Plant Cell* **16**: 1938–1950.

Lu Y, Eiriksson FF, Thorsteinsdóttir M, Simonsen HT. 2019. Valuable fatty acids in bryophytes-production, biosynthesis, analysis and applications. *Plants* **8**: 524.

Markham KR, Porter IJ. 1974. Flavonoids of the liverwort *Marchantia polymorpha*. *Phytochemistry* **13**: 1937–1942.

McConn M, Hugly S, Browse J, Somerville C. 1994. A mutation at the fad8 locus of *Arabidopsis* identifies a second chloroplast omega-3 desaturase. *Plant Physiology* **106**: 1609–1614.

Monte I, Franco-Zorrilla JM, García-Casado G, Zamarreño AM, García-Mina JM, Nishihama R, Kohchi T, Solano R. 2019. A single JAZ repressor controls the jasmonate pathway in *Marchantia polymorpha*. *Molecular Plant* **12**: 185–198.

Monte I, Ishida S, Zamarreño AM, Hamberg M, Franco-Zorrilla JM, García-Casado G, Gouhier-Darimont C, Reymond P, Takahashi K, García-Mina JM *et al.* 2018. Ligand-receptor co-evolution shaped the jasmonate pathway in land plants. *Nature Chemical Biology* **14**: 480–488.

Monte I, Kneeshaw S, Franco-Zorrilla JM, Chini A, Zamarreño AM, García-Mina JM, Solano R. 2020. An ancient COI1-independent function for reactive electrophilic oxylipins in thermotolerance. *Current Biology* 30: 962–971 e3.

Morimoto M, Kumeda S, Komai K. 2000. Insect antifeedant flavonoids from *Gnaphalium affine* D. Don. *Journal of Agricultural and Food Chemistry* 48: 1888–1891.

Peñuelas M, Monte I, Schweizer F, Vallat A, Reymond P, García-Casado G, Franco-Zorrilla JM, Solano R. 2019. Jasmonate-related MYC transcription factors are functionally conserved in *Marchantia polymorpha*. *Plant Cell* 31: 2491–2509.

Qi S-H, Zhang S, Qian P-Y, Wang B-G. 2008. Antifeedant, antibacterial, and antilarval compounds from the South China Sea seagrass *Enhalus acoroides*. *Botanica Marina* 51: 441–447.

Qi T, Huang H, Song S, Xie D. 2015. Regulation of jasmonate-mediated stamen development and seed production by a bHLH-MYB complex in *Arabidopsis*. *Plant Cell* 27: 1620.

Ran F, Hsu P, Lin C-Y, Gootenberg J, Konermann S, Trevino AE, Scott D, Inoue A, Matoba S, Zhang YI *et al.* 2013. Double nicking by RNA-guided CRISPR Cas9 for enhanced genome editing specificity. *Cell* 154: 1380–1389.

Reszczyńska E, Hanaka A. 2020. Lipids composition in plant membranes. *Cell Biochemistry and Biophysics* 78: 401–414.

Richards RL, Quackenbush FW. 1974. Alternate pathways of linolenic acid biosynthesis in growing cultures of *Penicillium chrysogenum*. *Archives of Biochemistry and Biophysics* 165: 780–786.

Sheard LB, Tan XU, Mao H, Withers J, Ben-Nissan G, Hinds TR, Kobayashi Y, Hsu F-F, Sharon M, Browse J *et al.* 2010. Jasmonate perception by inositol-phosphate-potentiated COI1-JAZ co-receptor. *Nature* 468: 400–407.

Shen B, Zhang W, Zhang J, Zhou J, Wang J, Chen LI, Wang LU, Hodgkins A, Iyer V, Huang X *et al.* 2014. Efficient genome modification by CRISPR-Cas9 nickase with minimal off-target effects. *Nature Methods* 11: 399–402.

Soriano G, Del-Castillo-Alonso MA, Monforte L, Nuñez-Olivera E, Martinez-Abaigar J. 2019. Acclimation of bryophytes to sun conditions, in comparison to shade conditions, is influenced by both photosynthetic and ultraviolet radiations. *Frontiers in Plant Science* 10: 998.

Soriano G, Del-Castillo-Alonso MA, Monforte L, Tomás-Las-Heras R, Martinez-Abaigar J, Nuñez-Olivera E. 2021. Developmental stage determines the accumulation pattern of UV-absorbing compounds in the model liverwort *Marchantia polymorpha* subsp. *ruderalis* under controlled conditions. *Plants* 10: 1–16.

Soukas A, Cohen P, Socci ND, Friedman JM. 2000. Leptin-specific patterns of gene expression in white adipose tissue. *Genes & Development* 14: 963.

Staswick PE, Tiryaki I. 2004. The oxylipin signal jasmonic acid is activated by an enzyme that conjugates it to isoleucine in Arabidopsis. *Plant Cell* 16: 2117–2127.

Sugano SS, Nishihama R. 2018. CRISPR/Cas9-based genome editing of transcription factor genes in *Marchantia polymorpha*. *Methods in Molecular Biology* 1830: 109–126.

Sugano SS, Nishihama R, Shirakawa M, Takagi J, Matsuda Y, Ishida S, Shimada T, Hara-Nishimura I, Osakabe K, Kohchi T. 2018. Efficient CRISPR/Cas9-based genome editing and its application to conditional genetic analysis in *Marchantia polymorpha*. *PLoS ONE* 13: e0205117.

Sumanta N, Imranul Haque C, Nishika J, Suprakash R. 2014. Spectrophotometric analysis of chlorophylls and carotenoids from commonly grown fern species by using various extracting solvents. *Research Journal of Chemical Sciences* 4: 63–69.

Thines B, Katsu L, Melotto M, Nin Y, Mandaokar A, Liu G, Nomura K, He SY, Howe GA, Browse J. 2007. JAZ repressor proteins are targets of the SCF(COI1) complex during jasmonate signalling. *Nature* 448: 661–665.

Wasternack C, Feussner I. 2018. The oxylipin pathways: biochemistry and function. *Annual Review of Plant Biology* 69: 363–386.

Weber H, Vick BA, Farmer EE. 1997. Dinor-oxo-phytodienoic acid: a new hexadecanoid signal in the jasmonate family. *Proceedings of the National Academy of Sciences, USA* 94: 10473–10478.

Woodson JD. 2019. Chloroplast stress signals: regulation of cellular degradation and chloroplast turnover. *Current Opinion in Plant Biology* 52: 30–37.

Supporting Information

Additional Supporting Information may be found online in the Supporting Information section at the end of the article.

Fig. S1 Scheme of OPDA, dn-OPDA and VLPUFAs biosynthesis in *Marchantia polymorpha*.

Fig. S2 Phylogenetic tree of *Arabidopsis thaliana* and *Marchantia polymorpha* desaturases proteins.

Fig. S3 Genotyping of Mp*fad5* alleles.

Fig. S4 C18 fatty acid measurements in *Marchantia polymorpha*.

Table S1 Chloroplast size measurements.

Table S2 Fatty acids measured in this study.

Table S3 Primers used in this study.

Please note: Wiley Blackwell are not responsible for the content or functionality of any Supporting Information supplied by the authors. Any queries (other than missing material) should be directed to the *New Phytologist* Central Office.